

X-690-74-344

PREPRINT

NASA TM X 70836

# INTERPLANETARY STREAM MAGNETISM - KINEMATIC EFFECTS

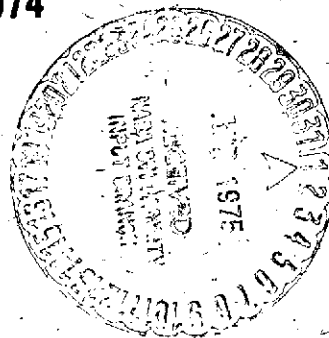
(NASA-TM-X-70836) INTERPLANETARY STREAM  
MAGNETISM: KINEMATIC EFFECTS (NASA) 37 P  
HC \$3.75 CSCL 03B

N75-19099

Unclas  
G3/90 13265

L. F. BURLAGA  
E. BAROUCH

NOVEMBER 1974



— GODDARD SPACE FLIGHT CENTER —  
GREENBELT, MARYLAND

For information concerning availability  
of this document contact:

Technical Information Division, Code 250  
Goddard Space Flight Center  
Greenbelt, Maryland 20771

(Telephone 301-982-4488)

"This paper presents the views of the author(s), and does not necessarily  
reflect the views of the Goddard Space Flight Center, or NASA."

Interplanetary Stream Magnetism — Kinematic Effects

L. F. Burlaga and E. Barouch\*  
Laboratory for Extraterrestrial Physics  
NASA/Goddard Space Flight Center

\* On leave from Service d'Electronique Physique, C.E.N. Saclay, and CNRS.  
NAS/NRC Senior Resident Research Associate.

## Abstract

The particle density, and the magnetic field intensity and direction, are calculated in corotating streams of the solar wind. It is assumed that the solar wind velocity is constant and radial and that its azimuthal variations are not too rapid. These assumptions are approximately valid between 0.1 and 1 AU for many streams. In the absence of streaming,  $n$  decreases as  $r^{-2}$  and  $B/n$  is relatively constant, although modified by corotation. Kinematic factors change the variation of  $n$  somewhat. Their effect on  $B$  is similar, but also depends on the initial orientation of  $\underline{B}$ . When our assumptions are valid, dynamic effects, which are considered briefly, will also change  $n$  and  $\underline{B}$  but to a lesser degree. By averaging over a typical stream, it is found that  $\langle B_r \rangle \sim r^{-2}$ , whereas  $\langle B_\phi \rangle$  does not vary in a simple way. Changes of field direction may be very large, depending on the initial angle; but when the initial angle at 0.1 AU is such that the base of the field line corotates with the sun the spiral angle is the preferred direction at 1 AU.

## 1. Introduction

The gas-dynamic properties of interplanetary streams have been extensively studied and were reviewed by Hundhausen (1972) and Burlaga (1974), but relatively little has been written about the theory of magnetic fields in streams. Sakurai (1971) considered a model of stationary, co-rotating streams which includes magnetic fields,  $\underline{B}$ , but neglects the reaction of  $\underline{B}$  on the velocity  $\underline{V}$ . Matsuda and Sakurai (1972) and Urch (1972) extended this work to include, to first approximation, the modifications of  $\underline{V}$  induced by the pressure gradients that are produced by the steepening of a speed profile. Exact numerical solutions for two-dimensional, stationary corotating streams were obtained by Nakagawa and Welck (1973) who introduced a temperature variation as well as a speed variation. All of these models consider an inner boundary at  $\approx 30 R_{\odot}$  and neglect the primary acceleration mechanism. We shall follow a similar approach; we consider that the streams begin as speed variations at  $0.1 \text{ AU} \approx 20 R_{\odot}$  and determine the effects of the steepening of the stream on the magnetic field and density between  $20 R_{\odot}$  and  $1 \text{ AU}$ .

The results of the stream-magnetism models mentioned above are all basically the same. They predict an enhancement of  $B$  in the leading part of the stream, a rarefaction in the trailing part and some perturbations of the magnetic field direction from the spiral angle. However, all of these models assume that  $\underline{B}$  is nearly radial at  $30 R_{\odot}$ , and thus fail to consider the large fluctuations of field direction about the spiral angle which are a general feature near  $1 \text{ AU}$ . Schatten

(1972) has briefly discussed the effect of speed gradients on the direction of  $\underline{B}$  and showed that the effect can be appreciable, but he considered only a few isolated events rather than stream profiles, and he did not examine magnetic field intensity variations.

In this paper we systematically examine the effects of the radial velocity profile in corotating streams on the magnetic fields between  $20 R_{\odot}$  and 1 AU, using the kinematic approximation,  $\frac{dV}{dt} = 0$  (i.e.,  $V =$  constant for any given volume element) and a variety of  $\underline{B}$  configurations on the inner boundary. Our approximation is valid for typical streams of moderate amplitude. It does not exactly describe very steep streams, but it allows one to examine a greater variety of conditions than one could explore with the relatively few solutions that one can compute in practice for more complicated dynamical models. Thus, the kinematic approximation provides considerable insight, which is our main objective. In any case, the zeroth order effects of the streams on  $\underline{B}$  are kinematic effects. For example, the magnetic field compression obtained in the dynamical models referenced above, is a kinematic effect; dynamical changes in  $\underline{V}$  are a consequence of this compression rather than the cause of it.

## 2. Basic Equations

### a) Approach

In practice, it is not possible to measure functions such as  $\underline{B}$  ( $x, y, z, t$ ) and  $V$  ( $x, y, z, t$ ) at every point in the solar wind. Rather, one measures functions of time, at one or two points in space, which to first approximation are the result of the passage of a continuous series

of volume elements moving radially past the observer. Thus, it is reasonable to adopt a Lagrangian point of view in which one follows volume elements moving on a radial line which joins the observer and the sun. Knowing the properties of each volume element as it moves from the sun to the observer, one can construct the time profiles that the observer sees as a result of the passage of a continuous train of such volume elements. This approach is used below.

### b) Velocity Gradients

As will be shown later, the changes in the properties of a volume element as it moves radially from  $(r)$  to  $(r + \Delta r)$  depend on the local gradients  $\frac{\partial V}{\partial r}$  and  $\frac{\partial V}{\partial \phi}$  at  $r$ , where  $\phi$  is the azimuthal angle from a reference point on the sun (See Figure 1). We obtain expressions for these quantities as follows.

Let us assume that at a distance  $r_0$  and an angle  $\delta$  in the frame rotating with the sun there is a stationary solar wind speed distribution  $V_0(\delta)$  a number density distribution  $n_0(\delta)$  and a magnetic field distribution  $B_0(\delta)$  (See Figure 1). As these distributions rotate past the observer-sun line, they generate time profiles which form a stream on that line. Let us define  $a(\delta)$  in the corotating frame as  $\frac{dV}{d\delta} = a(\delta)$ . Now let us consider a fixed frame of reference, in which the sun rotates with angular velocity  $\underline{\Omega} = \Omega \hat{z}$ . We assume that the solar wind velocity in the fixed frame is everywhere radial, as a first approximation. Plasma emitted at time  $t_1$  will reach  $r_1$  at time  $T_1 = t_1 + (r_1 - r_0)/V_1$ . At a time  $t_2$ , the sun will have rotated by an amount  $|\Delta\delta| = \Omega (t_2 - t_1)$ . A volume element emitted then will reach  $r_2$  at a time

$T_2 = t_2 + (r_2 - r_0)/V_2$ . If  $t_2 - t_1$  is sufficiently small,  $V_2 - V_1 = a|\delta| = a\Omega(t_2 - t_1)$ . Now consider volume elements arriving at  $r_1$  and  $r_2$  at the same time  $T$ ; for these,  $t_1 + (r_1 - r_0)/V_1 = t_2 + (r_2 - r_0)/V_2$ . Setting  $r_2 = r_1 + \Delta r$ , a little algebra shows that

$$\left. \frac{\Delta V}{\Delta r} \right|_{\psi = \text{const}} = \frac{a\Omega V_1 V_2}{V_2 [a\Omega(r_1 - r_0) - V_1 V_2]} \quad (1)$$

which becomes, in the limit  $\Delta r \rightarrow 0$ ,

$$\frac{\partial V}{\partial r} = - \left( \frac{a}{v} \right) \Omega \mu \quad (2)$$

where

$$\mu = \left[ 1 - \left( \frac{a}{v} \right) (r - r_0) \left( \frac{\Omega}{v} \right) \right]^{-1} \quad (3)$$

$$= \left[ 1 - \left( \frac{a}{v} \right) \frac{r - r_0}{R_c} \right]^{-1} \quad (3a)$$

with

$$R_c = v/\Omega \quad (3b)$$

Note that  $\Omega > 0$  and  $a > 0$  in the "rise" of a stream, so  $\mu > 1$  in a region where  $V$  increases with time. One can similarly calculate  $\frac{\partial V}{\partial \phi}$  as follows. Consider two volume elements moving with speeds  $V_2$  and  $V_1$  at  $r$  at  $T_1 = T_2$ . The difference between the departure times from  $r_0$  is  $t_2 - t_1 = (r - r_0)(V_2^{-1} - V_1^{-1})$ , during which time the sun rotates through an angle  $\Delta\phi_r = \Omega(t_2 - t_1)$ . Considering the geometry at  $r_0$ , one finds that  $V_2 = V_0 + a(\phi + \Delta\phi_r)$ . Collecting terms and taking the limits  $\Delta\phi \rightarrow 0$ ,  $\Delta t \rightarrow 0$ , one

obtains

$$\frac{\partial V}{\partial \varphi} = -a\mu \quad (4)$$

Note that equations (1), (3), and (4) are valid for all latitudes,  $\theta_0$ .

### c) Density Variations

We are now in a position to calculate the density variations in a volume element along its trajectory. Starting with the equation of continuity

$$\frac{1}{\rho} \frac{d\rho}{dt} = -\nabla \cdot \underline{v} = -\frac{\partial V}{\partial r} - \frac{2V}{r} \quad (5)$$

where  $\rho = nm$  is the mass density, and assuming that  $V$  is constant along a trajectory, so that  $\frac{d\rho}{dt} = V \frac{d\rho}{dr}$ , we obtain

$$\frac{V}{\rho} \frac{d\rho}{dr} = \frac{V}{n} \frac{dn}{dr} = -\frac{\partial V}{\partial r} - \frac{2V}{r} \quad (6)$$

Substituting (2) into this expression and integrating from  $r_0$  to  $r$  gives

$$n = n_0 \left( \frac{r_0}{r} \right)^2 \mu \quad (7)$$

Our first result, then, is that the density does not decrease with distance exactly as  $r^{-2}$ , unless  $a = 0$  (i.e. no stream); a kinematic correction factor is necessary, equal to  $\mu$  which is given by (3). The conditions under which (7) is valid are discussed in the Appendix. One can, however, state immediately that even if the density at the source is constant, independent of  $\delta$ , a volume element in which the speed is increasing ( $a > 0$ ) will have a higher density at  $r > r_0$  than an element

in which  $a = 0$ , since  $\mu > 1$  for  $a > 0$ . The variation of  $\mu$  with  $a/V$ , for observers at 0.3 AU, 1.0 AU, and 1.5 AU, is shown in Figure 2. The variation of  $\mu$  with  $r$  is also shown in Figure 2, for a few values of  $a/V$ . The compression or rarefaction of  $n$  implied by the variation of  $\mu$  has been noted by others in gas-dynamical models of streams (for references, see Hundhausen, 1972), but it is interesting to note that this is a kinematic effect. The dynamical effects tend to reduce the amount of compression or rarefaction; dynamical effects are the result of the density change rather than its cause.

#### d) Magnetic Field Variations

We wish to find the variations of  $\underline{B}(r)$  in a volume element along its trajectory. We start with the equation

$$\frac{\partial \underline{B}}{\partial t} = \nabla \times (\underline{V} \times \underline{B}) \quad (8)$$

which follows from one of Maxwell's equations with the frozen-field condition  $\underline{E} = -\underline{V} \times \underline{B}$ . Using a well-known identity for  $\nabla \times (\underline{V} \times \underline{B})$  with  $\nabla \cdot \underline{B} = 0$  and the definition of the convective derivative,  $d/dt = \partial/\partial t + \underline{V} \cdot \nabla$ , we obtain

$$\frac{d \underline{B}}{dt} = (\underline{B} \cdot \nabla) \underline{V} - \underline{B} (\nabla \cdot \underline{V}) \quad (9)$$

It is convenient to consider the variations of  $\underline{B}/n$  rather than  $\underline{B}$  directly.

$$\frac{d}{dt} \left( \frac{\underline{B}}{n} \right) = - \frac{\underline{B}}{n^2} \frac{dn}{dt} + \frac{1}{n} \frac{d \underline{B}}{dt} \quad (10)$$

Using (5) and (9) one finds that

$$\frac{d}{dt} \left( \frac{\underline{B}}{n} \right) = \frac{1}{n} (\underline{B} \cdot \nabla) \underline{V} \quad (11)$$

This is known as Walén's equation (Walén, 1946).

The LHS of (11) gives the change in  $B/n$  in a volume element which moves radially at constant speed relative to a fixed frame, as seen by an observer in the fixed frame. Let us consider a spherically symmetric coordinate system in which  $\hat{r}$  points radially away from the sun,  $\hat{\phi}$  is in the direction of motion of the planets, and  $\hat{\theta}$  is directed along  $\hat{\phi} \times \hat{r}$  (See Figure 1, or see Stratton, 1941, p. 52). The co-latitude is  $\theta$  ( $\sin \theta = 1$  in the ecliptic plane).

A general solution of Walén's equation is found in many textbooks on plasma dynamics, viz.,

$$\frac{\underline{B}}{n} = \frac{1}{n_0} \left( \underline{B}_0 \cdot \underline{\nabla}_0 \right) \underline{R} \quad (12)$$

where  $\underline{R}$  is the displacement vector of a volume element (We use  $\underline{R}$  instead of  $\underline{r}$  in this discussion to avoid confusion between Lagrangian and Eulerian coordinates). However, this is often given in an incorrect form or else the meaning is not fully explained. One of the clearest explanations of this equation is found in Batchelor (1970). Eq. (12) is the form of the solution given by Boyd and Sanderson (1969). Let the  $\phi$ ,  $\theta$  components of  $B/n$  be denoted as

$$f = B_\phi/n, \quad g = B_\theta/n \quad (13)$$

respectively and let  $f_0$  and  $g_0$  be the values at the inner boundary.

Since  $R = R\hat{r}$  in our case, (12) gives

$$\frac{\underline{B}}{n} = g_0 \left( \frac{\partial R \hat{r}}{\partial r_0} + R \frac{\partial \hat{r}}{\partial r_0} \right) + \frac{f_0}{r_0 \sin \theta} \left( R \frac{\partial \hat{r}}{\partial \phi} + \frac{\partial R \hat{r}}{\partial \phi} \right) \quad (14)$$

The values of the vector derivatives are  $\frac{\partial \hat{r}}{\partial \phi} = (\sin \theta) \hat{\phi}$  and  $\frac{\partial \hat{r}}{\partial r_0} = 0$ . The

other derivatives are obtained by differentiating the equation  $R = r_0 + V(r_0, \phi_0) t$  at a given  $t$ , noting that  $\frac{\partial V}{\partial r_0} = -\frac{r_0 \partial V}{V \partial \phi} = \frac{a}{V}$ . One obtains

$$\frac{\partial R}{\partial r_0} = 1 + \left(\frac{R-r_0}{V}\right) \left(\frac{\partial V}{\partial r_0}\right) = \frac{1}{\mu} \quad (15)$$

$$\frac{\partial R}{\partial \phi} = \left(\frac{R-r_0}{V}\right) \left(\frac{\partial V}{\partial \phi}\right) = -\frac{a}{V} (R-r_0) \quad (16)$$

Inserting these expressions into (14) replacing  $R$  by  $r$ , using (13) gives

$$\frac{\partial B}{\partial r} = \left( \frac{B_{r_0}}{n_0} \frac{1}{\mu} - \frac{a}{V} \frac{B_{\phi_0}}{n_0} \frac{r-r_0}{r_0 \sin \theta} \right) \hat{r} + \left( \frac{B_{\phi_0}}{n_0} \right) \frac{r}{r_0} \hat{\phi} \quad (17)$$

i.e.,

$$f = f_0 r / r_0 \quad (18)$$

$$g = \frac{g_0}{\mu} - f_0 \left( \frac{a}{V} \right) \frac{r-r_0}{r_0 \sin \theta} \quad (19)$$

Since there is confusion about the meaning and derivation of (12), it is instructive to derive the solution of (11) written in the particular form appropriate for our problem. We can set  $dt = dr/V$ , because we are following a volume element, whose speed is constant in our picture. Assuming that  $B_\theta = 0$  and that  $\underline{v} = V\hat{r}$ , (11) gives

$$\frac{dg}{dr} = \frac{g}{V} \frac{\partial V}{\partial r} + \frac{f}{r \sin \theta} \frac{1}{V} \frac{\partial V}{\partial \phi} \quad (20)$$

$$\frac{df}{dr} = \frac{f}{\sin \theta} \quad (21)$$

Using (2) and (4), Equation (21) can be integrated immediately, giving (18). Substituting this result into (20) and integrating gives (19).

One can write (17) in the form

$$\frac{\underline{B}}{n'} = \left( \frac{B_{r_0}}{n_0} + g_a \right) \underline{\hat{r}} + \mu \left( \frac{B_{\phi_0}}{n_0} \right) \frac{r}{r_0} \underline{\hat{\phi}} \quad (22)$$

where

$$n' = \frac{n}{\mu} = n_0 \left( r_0/r \right)^2 \quad (23)$$

is the "unperturbed" density at  $r$ , and

$$g_a = - \frac{a}{V} \frac{B_{\phi_0}}{n_0} \left( \frac{r-r_0}{r_0 \sin \theta} \right) \quad (24)$$

When  $a = 0$ ,  $g_a = 0$  and  $\mu = 1$ , and the components of  $\underline{B}$  are just  $B_{r_0} (r_0/r)^2$  and  $B_{\phi_0} (r_0/r)$ . If, furthermore,  $B_{\phi_0} = r_0 B_{\phi_0}/R_C$ , one has the result of Parker (1958) for a field line whose base corotates with the sun, assuming symmetric flow. In the case of a corotating stream, where  $a \neq 0$ ,  $B_{\phi}$  is enhanced by the factor  $\mu$ , and  $B_r$  is augmented by an amount proportional to  $a$  and to  $B_{\phi_0}$ . When the field is initially radial,  $\underline{B} = B_{r_0} (r_0/r)^2$ ; in our approximation, the streaming does not modify  $\underline{B}$  in this case. For the rather unlikely case of an initially azimuthal field, a radial component whose magnitude can be calculated from (22) is produced by the velocity shear in the stream.

### 3. STREAMS AT 1 AU

Let us consider an observer at a fixed point at 1 AU and ask what he should measure as a corotating stream moves past him. For simplicity, let us begin by considering a stream whose speed profile at 0.1 AU is  $V = V_0 + \Delta V \cos 4\delta$ , where  $V_0 = 400$  km/s and  $\Delta V = 75$  km/(sec.rad.) Such a profile corresponds to a minimum speed of 325 km/sec and a maximum speed of 475 km/sec, and to 4 streams per solar rotation. This approximates the characteristics of the streams observed by IMP 1 (Wilcox and Ness, 1965) and a stream which Hundhausen (1972) chose to fit with his gas-dynamic model. It may be regarded as a representative stream (e.g. see Hundhausen, 1972; Burlaga, 1974). We assume that the density and magnetic field intensity are constant at the inner boundary (0.1 AU), being  $800/\text{cm}^3$  and  $500\gamma$  respectively. The results which follow refer to streams defined in this way, which we shall call our "standard" values.

In general, both the direction and magnitude of  $\underline{B}$  will depend on  $\underline{B}_0$  at  $r = r_0$ . Let us consider three cases: 1) the base of the field line in each volume element corotates with the sun, so that  $\phi_0 = \tan^{-1}(B_r/B_\theta) = \tan^{-1}(-r_0/R_c)$ ; 2) the field direction is the same for all volume elements at  $r_0$ , equal to  $93^\circ$ ; 3) the field direction is constant, equal to  $99^\circ$ . For such streams, the maximum value of the parameter  $\mu = 1/[1 - \frac{a}{V}(r-r_0)/R_c]$  = 3 (where  $r = 1$  AU,  $r_0 = 0.1$  AU,  $R_c = 1$  AU/rad, and  $\frac{a}{V} = 4\Delta V/V_0 = .75$ ). The time profiles of  $V$ ,  $n$ ,  $\underline{B}$ , and  $\phi$  which an observer at 1 AU should see, according to our model, are shown in Figure 3. The speed profile is asymmetric because the fast elements overtake the slow elements ahead of them; the density is enhanced where  $V$  is increasing, with a maximum

value three times the ambient value; and the density is reduced in the region where  $V$  is decreasing. This is in quantitative agreement with observations and with the results of previously published, gas-dynamic models. In addition, our model predicts that the magnetic field intensity is enhanced in the region of increasing  $V$ , with a maximum a few times the ambient value at 1 AU; the magnetic field intensity is depressed below the ambient value at 1 AU in the region of decreasing  $V$ ; and the magnetic field direction shows deviations from the spiral direction which vary systematically with the speed profile. Similar results were obtained from the non-linear MHD models of Matsuda and Sakurai (1972) and Nakagawa and Welck (1973) for a field which is parallel to the velocity in the corotating system. Our model shows quite clearly that these effects are kinematic rather than dynamical, and it has the advantage of allowing us to compute rather simply the effects of arbitrary field orientations near the inner boundary.

Figure 3 shows that the magnitude and direction of  $\tilde{B}$  at 1 AU depends sensitively on  $\Phi_0$  at  $r_0$ . For Parker's boundary condition ( $\Phi_0 = \tan^{-1}(-r_0/R_c)$ ), one finds an enhancement of  $B$  in the region of increasing  $V$ , the maximum being  $\approx 4$  times the value which would have occurred if  $a/V$  were zero (see Figure 3). The value of  $\Phi_0$  corresponding to the mean speed (400 km/s) in this case is  $\Phi_0 = 96^\circ$  and  $B_{\phi_0} \approx B_0 \cos 96^\circ = B_0 \sin(90^\circ - \Phi_0) \approx -6^\circ \times (\pi/180) \times B_0$ . If  $\Phi_0$  is constant equal to  $93^\circ$ , the enhancement is smaller because  $B_{\phi_0}$  is smaller by a factor of 2 ( $B_{\phi_0} \approx -3^\circ \times (\pi/180) \times B_0$ ) while  $B_{r_0} \approx B_0 \sin 96^\circ \approx B_0$  does not change significantly. Similarly, if  $\Phi_0$  is constant equal to  $99^\circ$ ,  $B_{\phi_0}$  is larger because  $B_{\phi_0}$  is

larger while  $B_r$  remains approximately  $B_0$ . There is a corresponding change in angles. For Parker's boundary condition, one sees the angle change rapidly in the interaction region from a "tight spiral" where  $V$  is low to a "loose spiral" where  $V$  is high. For  $\phi_0 = 93^\circ$  a similar change occurs, but in this case the field is generally more radial because of the smaller  $B_\phi$ . Similarly, for  $\phi_0 = 99^\circ$ , the field is less radial because  $B_\phi$  is larger.

Observations show that the field is often at a large angle to the spiral direction. One possible interpretation is that it is the image of large deviations from the radial direction at the source. This leads us to study kinematic effects on magnetic fields of arbitrary initial orientation. We have calculated  $\phi$  and  $|\underline{B}|/n$  at 1 AU for a volume element starting at 0.1 AU as a function of the initial angle  $\phi_0$  for different values of  $a/V$ . The results are shown in Figures 4 and 5.

Figure 4 shows  $\phi$  at 1 AU as a function of  $\phi_0$  at 0.1 AU. The dashed curve is the case  $a = 0$ . The variation of  $\phi$  is due to the rotation of  $\underline{B}$  with  $\phi_0$ , since  $B_{r_0} = B_0 \sin \phi_0$  and  $B_\phi = B_0 \cos \phi_0$  (see (22)). When  $\underline{B}_0 = B_0 \hat{r}$  ( $\phi_0 = 90^\circ$ ),  $\underline{B}/n^1 = B_0/n_0 \hat{r}$  ( $\phi = 90^\circ$ ). When  $\phi_0 = 96^\circ$ ,  $\phi_0 = 138^\circ$ , corresponding to the classical spiral result. When  $B_0 = B_0 \hat{\phi}$  ( $\phi_0 = 180^\circ$ ),  $\phi$  is also  $180^\circ$ , i.e., an initially azimuthal field remains azimuthal if  $a/V = 0$ . As  $\phi_0$  increases from  $96^\circ$  to  $180^\circ$ , the field becomes more azimuthal because  $B_\phi$  is increasing while  $B_{r_0}$  is decreasing. When  $a \neq 0$ , the shape of  $\phi$  ( $\phi_0$ ) is similar to that for  $a = 0$ , but it is displaced vertically and distorted somewhat (see Figure 4). This is most simply understood by considering  $\phi_0 = 180^\circ$  ( $B_{r_0} = 0$ ).

Eqs. (22) and (24) show that when  $a/V > 0$  the velocity shear twists the field so that there is a component  $|A|\hat{r}$  which yields  $\Phi < 180^\circ$ . When  $a/V < 0$  the shear is in the opposite direction ( $-\hat{r}$ ) and  $\Phi > 180^\circ$ .

The dependence of  $|\underline{B}|/n = B/n$  on  $\Phi_0$  is shown for our standard stream in Figs. 5a and 5b. Note that  $B/n(\Phi_0 + 180^\circ) = B/n(\Phi_0)$ , meaning that  $B/n$  does not depend on the sense of  $\underline{B}_0$  and we need only consider  $0^\circ \leq \Phi_0 \leq 180^\circ$ . When  $a = 0$  ( $A = 0$ ),  $B/n^{\perp} = (B_0/n_0) \sin \Phi_0 \hat{r} + (B_0/n_0)(r/r_0) \cos \Phi_0 \hat{\phi}$  and the variation of  $B/n$  is simply "sinusoidal" with a maximum at  $\Phi_0 = 0^\circ, 180^\circ$ . When  $A \neq 0$ , the position and magnitude of the maxima and minima change somewhat, as can be seen by considering (22). If one interprets visual coronal features as delineating magnetic field lines, it is to be expected that the field will be nearly radial most of the time so that values of  $\Phi_0$  close to  $90^\circ$  and  $270^\circ$  in Figures 4 and 5 are the most interesting.

#### 4. VARIATIONS WITH DISTANCE FROM THE SUN

##### a) Time Profiles at 0.3 AU

Consider a stream which at 0.1 AU is characterized by  $V = V_0 + \Delta V \cos(4\delta)$ ,  $V_0 = 400$  km/s,  $\Delta V = 75$  km/s,  $B_0 = 500\gamma$ , and  $n_0 = 800$  cm<sup>-3</sup>. The time profiles of such a stream at one AU were shown in Figure 3 and were discussed in the preceding section. The time profiles of this stream at 0.3 AU are shown in Figure 6. The asymmetry of the speed profile is scarcely noticeable, but it is sufficient to produce a 30% variation in the density. There is a modulation in  $B$  which depends on  $\Phi_0$ , being  $\approx 15\%$  for  $\Phi_0 = \tan^{-1}(-r_0/R_c)$ , somewhat larger for a more azimuthal initial field ( $\Phi_0 = 99^\circ$ ), and somewhat smaller for a more radial field ( $\Phi_0 = 93^\circ$ ). The variations in the direction of  $\tilde{B}$  at 0.3 AU also depend on  $\Phi_0$ . When  $\Phi_0 = \tan^{-1}(-r_0/R_c)$  the angle is more azimuthal at low speeds and more radial at high speeds. However, this is a small change and occurs across the interaction region, which is broad at 0.3 AU because the stream has not steepened much as yet. Consequently, the change in  $\Phi$  due to the stream is difficult to observe at 0.3 AU. The general conclusion from Figures 3 and 6 is that although there are qualitative similarities between the stream profiles at 0.3 and 1.0 AU, the quantitative differences are appreciable—the perturbations in  $n$ ,  $B$ , and  $\Phi$  are relatively small at 0.3 AU but are large, obviously non-linear features at 1.0 AU. If large perturbations in  $B$  are observed near 0.3 AU, it is safe to assume that they are not due to corotating streams, and alternative causes, such as variations in the source field or fields in flare-associated streams (Barouch et al., 1973), should be considered.

b) Variation of  $\langle B_r \rangle$  and  $\langle B_\phi \rangle$  with  $r$

Radial variations of  $B_r$  and  $B_\phi$  in the solar wind have been reported by several observers. The custom is to compute  $\langle B_r \rangle$  and  $\langle B_\phi \rangle$  over  $\approx 27$  day intervals for several different  $r$  and to compare the results with Parker's model for a homogeneous solar wind which predicts  $B_r \sim r^{-2}$  and  $B_\phi \sim r^{-1}$ . The averaging approach and comparison with Parker's model can be misleading, however, because of the presence of streams and the possible variability of the field near the sun.

Consider a solar wind made up of our "standard" streams and consider  $\sin \theta = 1$ . We have computed time averages of  $B_\phi$  and  $B_r$  over these streams at several different distances,  $r$ , for  $\phi_0 = 93^\circ$ ,  $99^\circ$ , and  $\phi_0 = \tan^{-1} (-r_0/R_c)$ . The results are shown in Figure 7.

We find that  $\langle B_r \rangle \sim r^{-2}$  with no noticeable dependence on  $\phi_0$ . Equation (22) shows that, this is because when  $\phi_0$  is near  $90^\circ$   $B_r \approx n^1 \chi$   $B_{r_0}/n_0 = (r_0/r)^2 B_0 \cos \alpha \approx B_0 (r_0/r)^2$ , where  $\alpha \equiv \phi_0 - 90^\circ$  is a small angle. An  $r^{-2}$  dependence of  $\langle B_r \rangle$  has been reported by Burlaga and Ness (1968) and Villante and Mariani (1975) between 0.8 AU and 1 AU, by Behannon et al. (1974) between 0.46 AU and 1 AU, and by Smith (1974) between 1 AU and 5 AU. (The Mariner 4 observations between 1 AU and 1.5 AU (Coleman et al., 1965) and the Mariner 5 observations between 0.7 AU and 1 AU (Rosenberg, 1970; Rosenberg and Coleman, 1973) did not give an  $r^{-2}$  dependence, however; the reason for this is not known).

The behavior of  $\langle B_\phi \rangle$  is more complicated than that of  $\langle B_r \rangle$ . Our model shows that if  $\phi_0$  is constant throughout the stream or equal to  $\tan^{-1} (-r_0/R_c)$ , then  $\langle B_\phi \rangle \sim r^{-1}$ , but it also shows that  $\langle B_\phi \rangle$  is very sensitive to  $\phi_0$ . The reason is apparent from (22) which shows that

$B_{\phi} = n^1 (B_{\phi_0}/n_0)(r/r_0) \mu = \mu B_0 \sin \alpha (r_0/r) \approx \mu B_0 (r_0/r) \alpha$ ; i.e.,  $B_{\phi}$  varies as  $r^{-1}$ , but it is also directly proportional to  $\phi_0 - 90^\circ$ . Thus, variations in  $\phi_0$  are reflected proportionally in  $B_{\phi}$ . When  $\phi_0$  takes values between  $93^\circ$  and  $99^\circ$ , for our standard stream,  $\langle B_{\phi} \rangle$  can lie somewhere in the shaded area of Fig. 7. Measured values of  $\langle B_{\phi} \rangle$  depend on the value of  $\phi_0$  near the sun, and on its fluctuations, as well as on the stream parameters. As the initial value and its statistical properties may depend on time and on position, measurements of  $\langle B_{\phi} \rangle(r)$  performed during an extended period may well deviate significantly from an  $r^{-1}$  dependence. Several groups have reported on the radial dependence of  $\langle B_{\phi} \rangle$ , expressed in the form  $\langle B_{\phi} \rangle \propto r^{-\gamma}$ . Villante and Mariani find  $\gamma = 2.5 \pm 2$ , Behannon et al. (1974) find  $\gamma = 1.22$  or  $1.4$ , Smith (1974) finds results consistent with  $\gamma = 4$ , and Rosenberg and Coleman found  $\gamma = 1.85$  aboard Mariner 5 and  $1.22$  aboard Mariner 4. These apparently conflicting results may well find their explanation in different distributions of  $\phi_0$  during the time of these measurements.

#### d) Map of Magnetic Field Intensity

Figure 8 shows "equi-intensity" contours of  $B/B_0$  between 0.1 AU and 1.0 AU, computed for our standard stream ( $V = 400 + 75 \cos 4\delta$ ) with  $\phi_0$  given by Parker's boundary condition.  $B_0$  is the intensity that would be obtained if  $a = 0$ . The intensification of  $B$  in the region of increasing  $V$  is evident, as is the depression in the region of decreasing  $V$ . The depression is relatively small everywhere. The enhancement is large and increases rapidly near 1 AU.

Figure 8 was obtained by computing  $B(t)$  profiles at 20 different values of  $r$ , plotting  $\frac{B}{B_0}$  along circles with the various radii (assuming corotation), and connecting points with equal values of the ratio of  $B(r)/B_0(r)$ . There is some uncertainty in the shapes of the contours where the curvature is large, due to the finite mesh size that was used (0.05 AU), but generally, Figure 8 conveys a reasonably accurate image of the magnetic field intensity pattern in a corotating stream.

## 5. SUMMARY AND DISCUSSION

We have presented a theory for the kinematic behavior of magnetic fields in streams in the solar wind between 0.1 AU and 1 AU. The theory is based on the assumption that  $\underline{v}$  is constant and radial for any given volume element in the region considered and that the local speed gradients are not too large. This breaks down beyond 1 AU and for parts of the steepest streams at 1 AU, but generally it is a very good approximation for examining the behavior of  $\underline{B}$  in the region inside 1.0 AU. By starting with speed profiles rather than temperature profiles, we fail to obtain well-known features concerning the temperature, but these have been adequately studied elsewhere and are not important as regards the kinematics of the magnetic field.

The magnetic field variations are in the same sense as the density variations, but the ratio  $B/n$  depends strongly on the initial orientation,  $\Phi_0$ , and the velocity gradient. The directional changes incurred by  $\underline{B}$  are quite complex to describe, but are very sensitive to  $\Phi_0$ ; for  $\Phi_0$  near  $90^\circ$ . They are the result of the compression and "shear" of the  $B_\phi$  component of  $\underline{B}$ , which are caused by the velocity gradients of the stream.

The implications of these calculations to the theory of cosmic ray propagations may be mentioned. Streams are a permanent feature of the interplanetary medium, and we expect regions of relatively intense magnetic field to be associated with each stream. These must be taken into account in cosmic ray propagation processes in a different manner than the usual diffusion-type calculations, as has already been pointed out. (Barouch and Raguideau, 1970; Barouch and Burlaga, 1974).

Motivated by the availability of data obtained between 0.46 and 1 AU by the Mariner-Venus-Mercury spacecraft and the forthcoming data to 0.3 AU from the Helios spacecraft, we have examined how the magnetic field should change in the ecliptic plane between 0.3 AU and 1 AU as a result of stream kinematics. At 0.3 AU, the time variations are nearly linear, with small enhancements and depressions in  $B$  and  $n$  and with very small changes in  $\Phi$  across the stream. These variations grow nonlinearly as one approaches 1 AU. The growth depends on the field direction,  $\Phi_0$  at the inner boundary. It has been the practice to compute time averages of  $B_r$  and  $B_\phi$  at different distances and compare them with the  $r^{-2}$  and  $r^{-1}$  variations predicted by the classical spiral model for a homogeneous wind with no streams. Averaging over a model stream, we find that  $\langle B_r \rangle \sim r^{-2}$  and is insensitive to  $\Phi_0$ , in agreement with the spiral model and with some observations; but we find that  $\langle B_\phi \rangle$  is very sensitive to  $\Phi_0$  and will not generally be proportional to  $r^{-1}$  if  $\Phi_0$  changes in the stream, which may explain why the observations do not show an  $r^{-1}$  dependence and vary among themselves. The field direction is very sensitive to the orientation near the sun and small departures from the "spiral angle",  $\Phi_0 = \tan^{-1} (-r_0/R_c)$ , cause a large spread about the spiral angle at  $r > r_0$ , the spread increasing with  $r$ . Thus, the observed variation in the direction of  $\underline{B}$  at 1 AU might be partly the result of relatively small fluctuations in the direction of  $\underline{B}$  near the sun.

#### REFERENCES

- Barouch, E., and Raguideau, J., 1970, Astron. and Astrophys., 9, 146.
- Barouch, E., Engelmann, J-J., Gros. M. and Masse, P., 1973, Proc. 13th Intl. Conf. Cosmic Rays, 2, 1426.
- Barouch, E., and Burlaga, L. F., 1974, J. Geophys. Res., to be published.
- Batchelor, G. K., 1970, An Introduction to Fluid Dynamics, ch. 5.3 (Great Britain: Cambridge University Press).
- Boyd, T. J. and Sanderson, J. J., 1969, Plasma Dynamics, p. 62 (New York: Barnes and Noble, Inc.).
- Behannon, K. W., Lepping, R. P., Ness, N. F., and Whang, Y. C., 1975, International Symposium on Solar-Terrestrial Physics, Vol. 1, p. 178.
- Burlaga, L. F., 1974, Space Science Rev. (in press).
- Burlaga, L. F., and Ness, N. F., 1968, Can. J. Phys., 46, 5962.
- Coleman, P. J., Jr., Smith, E. J., Davis, L., Jr., and Jones, D. E., 1969, J. Geophys. Res., 74, 2826.
- Hundhausen, A. J., 1972, Solar Wind and Coronal Expansion, (New York: Springer-Verlag).
- Hundhausen, A. J., 1973, J. Geophys. Res., 78, 1528.
- Matsuda, T., and Sakurai, T., 1972, Cosmic Electrodynamics, 3, 97.
- Nakagawa, Y., and Welck, R. E., 1973, Solar Physics, 32, 257.
- Parker, E. N., 1963, Interplanetary Dynamical Processes (New York: Interscience publishers).
- Rosenberg, R. L., 1970, J. Geophys. Res., 75, 5310.
- Rosenberg, R. L., and Coleman, P. J., Jr., 1963, The Radial Dependence of the Interplanetary Magnetic Field: 1.0-0.7 AU, publ. no. 1196-26, Instit. of Geophys. and Planet. Phys., UCLA.

- Sakurai, T., 1971, Cosmic Electrodynamics, 1, 460.
- Smith, E. J., 1974, Proceedings of the 3rd Asilomar Conference on the Solar Wind, Los Angeles, 1974.
- Stratton, J., 1941, Electromagnetic Theory, (New York: McGraw-Hill Book Company, Inc.).
- Urch, I. H., 1972, Cosmic Electrodynamics, 3, 316.
- Villante, U., and Mariani, F., 1975, Geophys. Res. Letters, in press.
- Walén, C., 1946, Arkiv Mat. Astron. Fysik, 33A, No. 18.
- Wilcox, J. M., and Ness, N. F., 1965, J. Geophys. Res., 70, 5793.

## FIGURES

1. This illustrates the geometry and defines angles. Note that  $V(\delta)$  is stationary in the corotating frame.
2. (top)  $\mu$  ( $a/V$ ) at 0.3 AU, 0.5 AU, and 1.5 AU (bottom)  $\mu$  ( $R$ ) between 0.1 AU and 1 AU for  $a/V = 0, \pm 0.4, \pm 0.7$ .  $\mu$  is  $n(r)/n_0$  where  $n_0$  is the density at 0.1 AU.
3. Time profile of a stream at 1 AU. The magnetic field intensity,  $B$ , and direction  $\phi$ , depend on the angle  $\phi_0$  at  $r = 0.1$  AU, but  $n$  is independent of  $\phi_0$ .
4.  $\phi$  at 1 AU ( $\phi_1$ ) versus  $\phi_0$  at 0.1 AU for  $a/V = 0, \pm 0.4, \pm 0.7$ .
5.  $B/n$  versus  $\phi_0$ . a)  $a/V > 0$ , b)  $a/V < 0$ .
6. Time profile of a stream at 0.3 AU.
7.  $\langle B_r \rangle$  and  $\langle B_\phi \rangle$  averaged over the time profile of a "standard" stream as a function of distance from the sun,  $R$ .  $\langle B_r \rangle \sim R^{-2}$ , but  $\langle B_\phi(R) \rangle$  depends on  $\phi_0$ .
8. Contour map of  $B/B_{a=0}$  for our "standard" stream.  $B_{a=0}$  is the value of  $B(r, \phi)$  that would be measured in the absence of a stream. The view shown is in the ecliptic plane.

APPENDIX

Validity of the Kinematic Approximation

All of the results discussed above are based on the kinematic approximation, in which we set the right hand side of the radial component of the momentum equation

$$\rho \frac{dV}{dt} = -\frac{\partial p}{\partial r} - \frac{\partial}{\partial r} \left( \frac{B^2}{8\pi} \right) + \left( \frac{B \cdot \nabla}{4\pi} \right) B \quad \text{A.1}$$

equal to zero. Neglecting the  $(B \cdot \nabla) B_r$  term is justifiable because it is on the order of the ratio of the size of the interaction region to the radius of curvature of the spiral field line, which is  $\ll 0.1$ . Since we are interested only in an order of magnitude estimate of the ratio of the RHS to the LHS of (A.1), we can make the following approximations to

estimate the size of the RHS of (A.1);  $B = \frac{B_1 \rho}{\rho_1}$ ,

and  $P = P_1 (\rho/\rho_1)^2$  (where  $P$  is the pressure) which is an adiabatic

law with  $\gamma = 2$ . Let us divide both sides of A.1 by  $\rho$  and set  $\frac{d}{dt} \approx V \frac{d}{dr}$ ,

which is valid

when  $V = \text{constant}$ . The RHS

is then  $\frac{-V_{M_1}^2}{\rho_1} \frac{d\rho}{dr}$ , where  $V_{M_1}^2 = V_s^2 + V_A^2 = (2P_1/\rho_1) + (B_1^2/(4\pi\rho_1))$  at 0.1 AU; here,  $V_s$  and  $V_A$  are the sound speed and Alfvén speed respectively.

The equation can then be integrated to give  $V_1^2 - V_0^2 \approx -V_{M_1}^2 (1 - \rho_0/\rho_1)$ ,

where the subscript zero refers to the inner boundary. Since  $\rho_1 =$

$\mu \rho_0 (r_0/r)^2$ ,  $V^2 = V_0^2 - 2V_{M_1}^2 (\mu - (r/r_0)^2)/\mu$ . Let  $\bar{V}_{M_1}^2 = V_{M_1}^2/\mu$  which is the magnetoacoustic speed at 1 AU in the absence of distortions due

to streams ( $a = 0$ ). Then

$$V^2 = \left( V_0^2 + 2 \bar{V}_{M_1}^2 \right) - 2\mu \bar{V}_{M_1}^2 \quad \text{A.2}$$

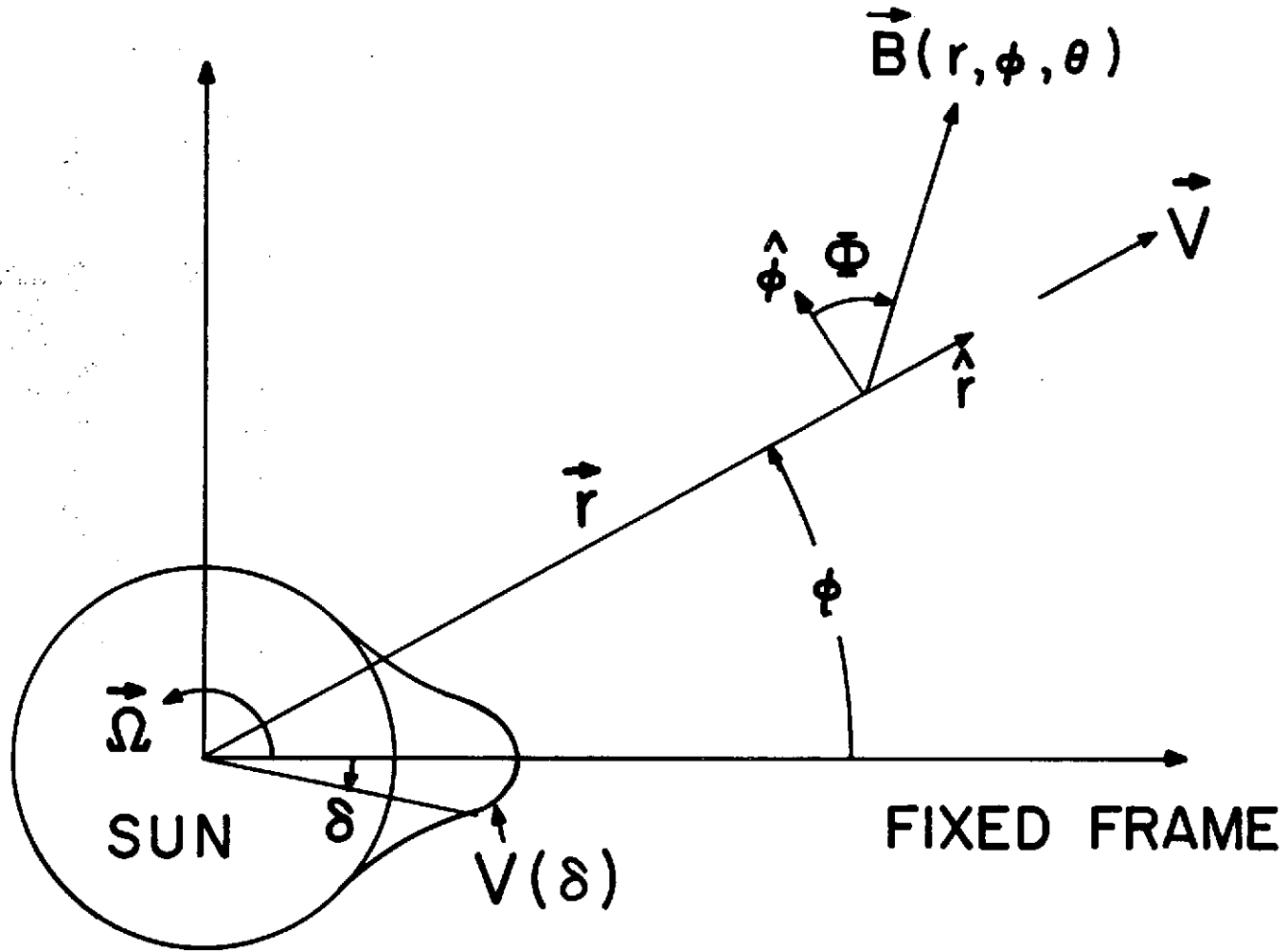
The second term on the RHS of (A.2) is the result of an acceleration of the volume element by the ambient gradients of  $p$  and  $B$ , and the third term represents the effect of a stream. We consider that the effect of a stream is negligible if  $v_{M_1}^2 \mu_1 \ll 0.0 v_0^2$ . For the parameters that we have been using,  $\bar{v}_{M_1}^2 \mu_1 \ll 2 \times 10^4 \text{ (km/s)}^2$  and  $v_0^2 \approx 2 \times 10^5 \text{ (km/s)}^2$ , so the effects of streams on  $V$  (the radial component of the velocity) can indeed be neglected to first approximation up to 1 AU if  $|\frac{a}{\bar{v}}| \ll 0.7$ . This is true for most streams  $\ll 1.0$  AU, but the approximation probably breaks down for the steepest streams at 1 AU, and it cannot be used much beyond 1 AU for most streams.

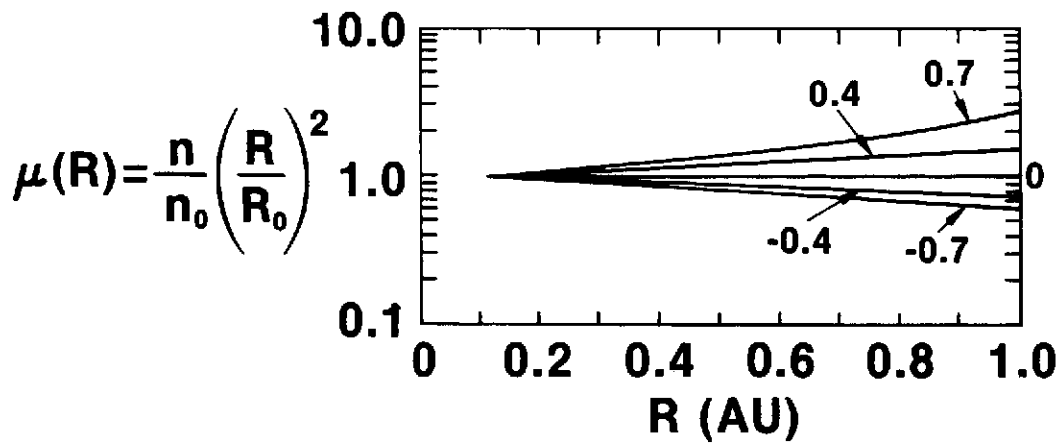
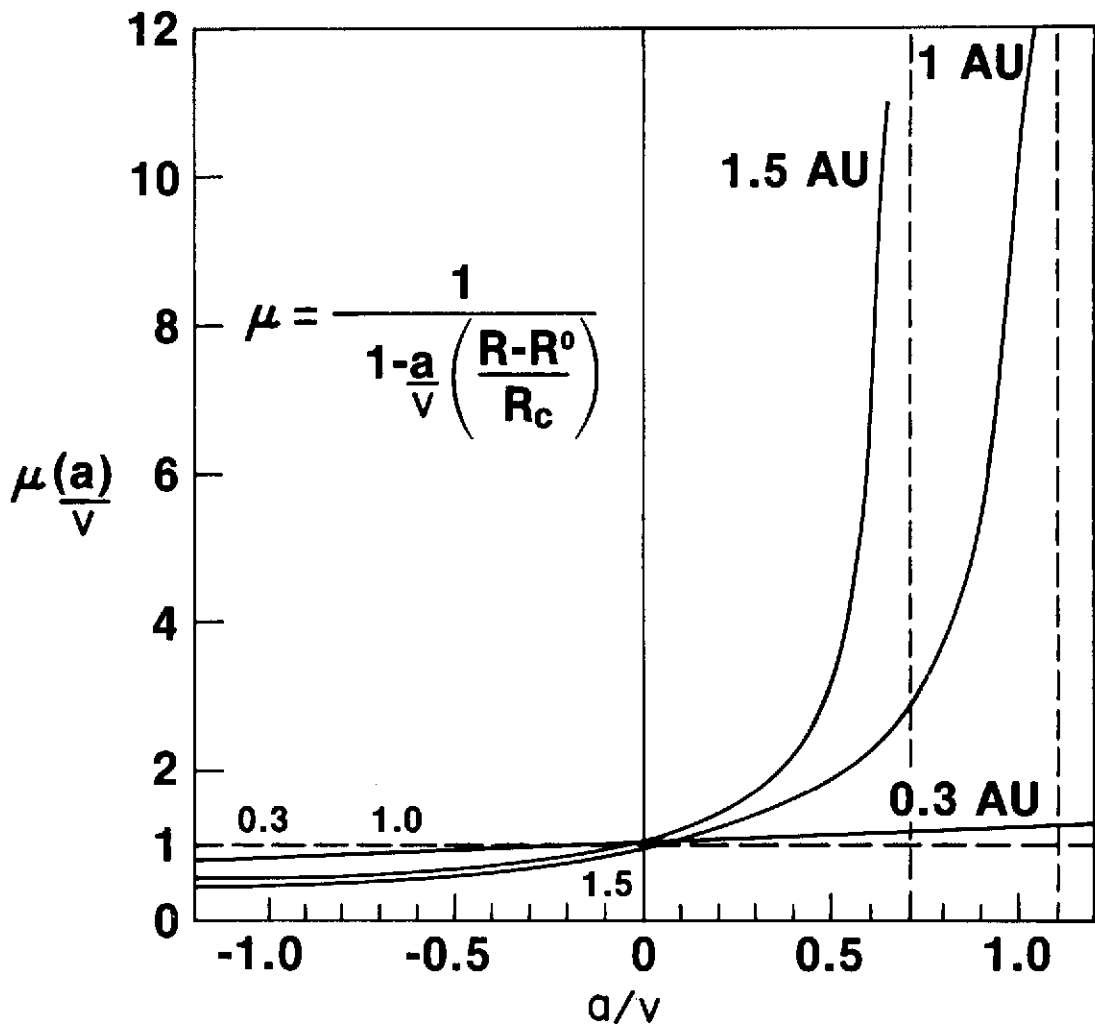
It is interesting to note from (A.2) that when our approximation does break down, energy is extracted from the flow to provide the potential energy in the pressure pulse, the decrease in  $V$  being greatest where  $\mu$ , i.e. the density enhancement, is greatest. This implies that the speed profile which is computed assuming  $\frac{dV}{dt} = 0$  will be altered such that it is steeper at 1 AU, and the density enhancement will appear to be closer to the front of the resulting stream.

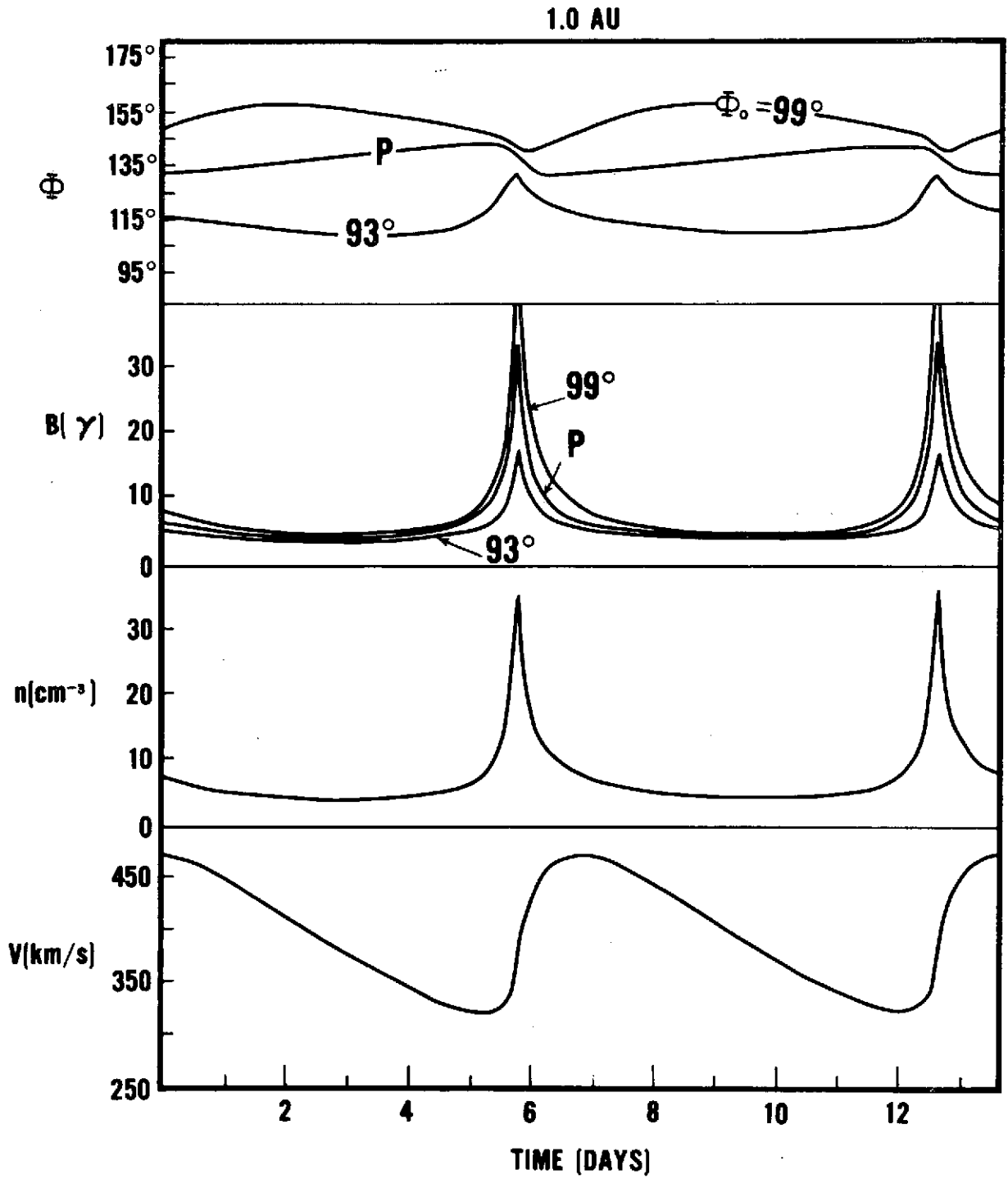
### Acknowledgements

One of us (E.B.) is indebted to the National Academy of Sciences for a Senior Resident Research Associateship, and to N. F. Ness for his kind hospitality at the Laboratory for Extraterrestrial Physics, NASA/Goddard Space Flight Center. We are deeply indebted to E. C. Roelof for helpful suggestions and corrections, as well as to A. J. Klimas and other colleagues for discussions and criticism. Technical assistance by J. Hodge and J. Phibbons is acknowledged with gratitude.

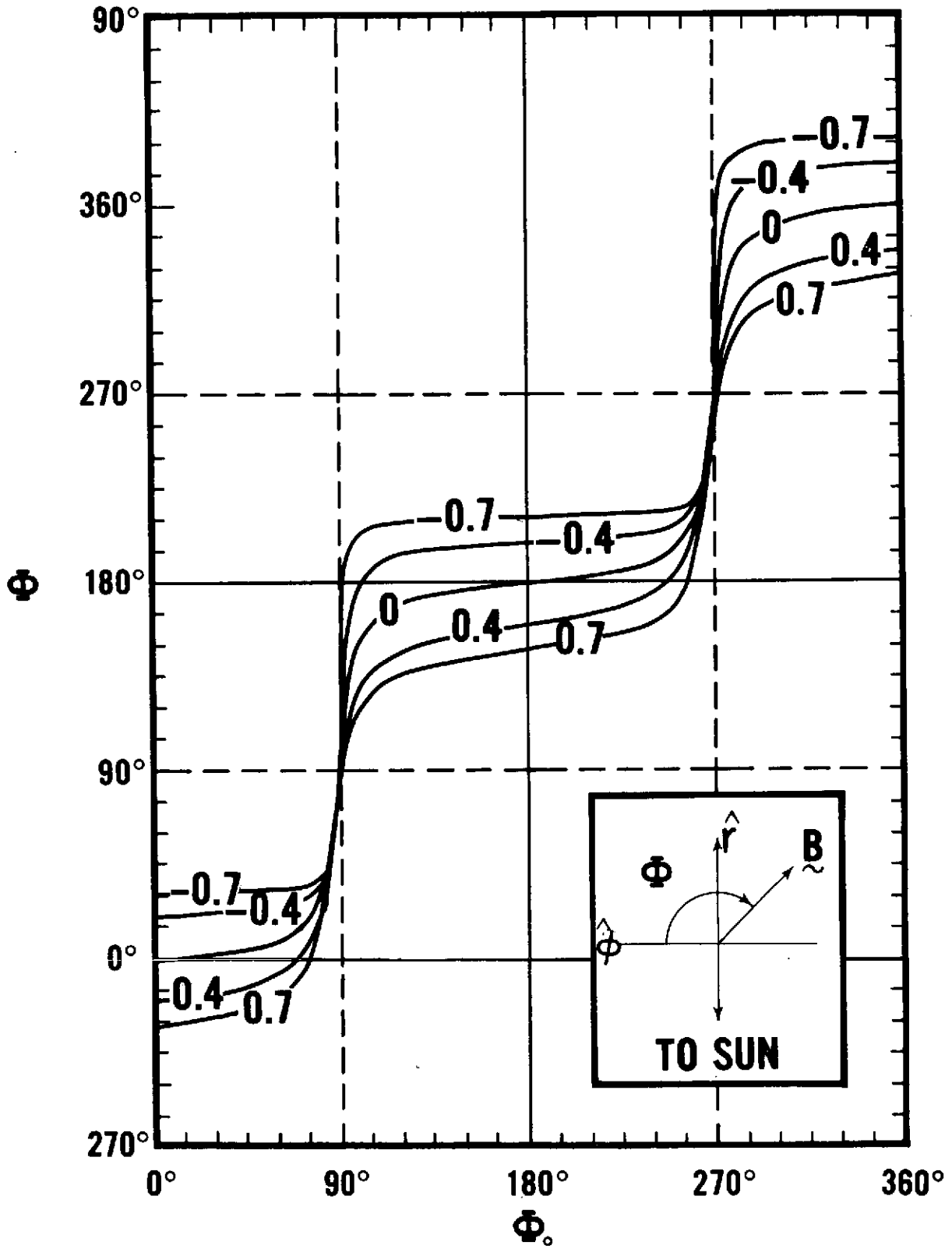
**REPEATING PAGE BLANK NOT FILMED**

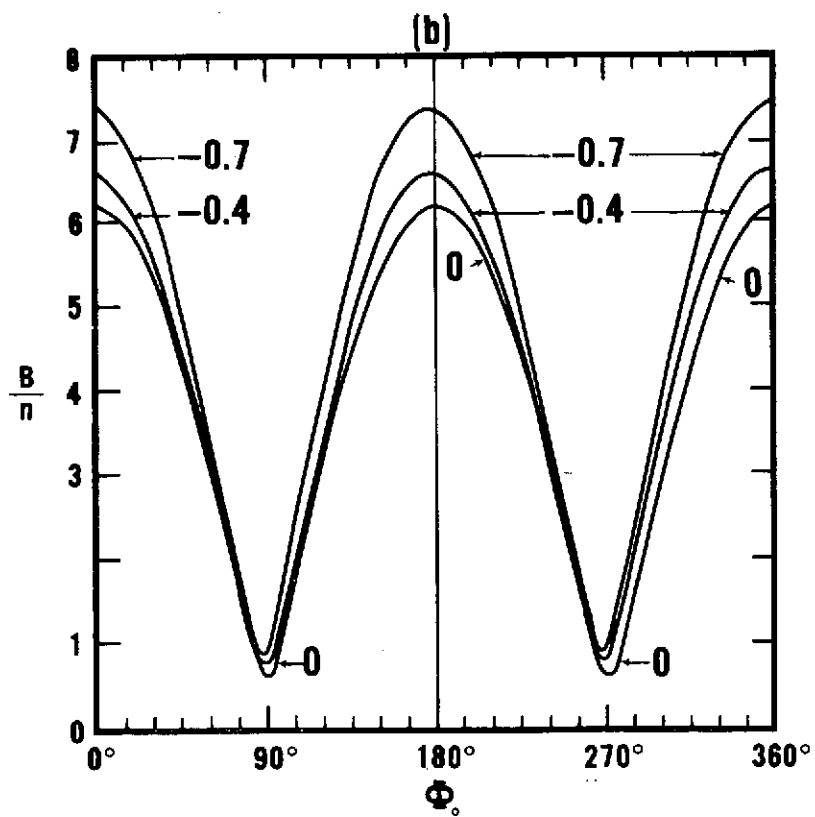
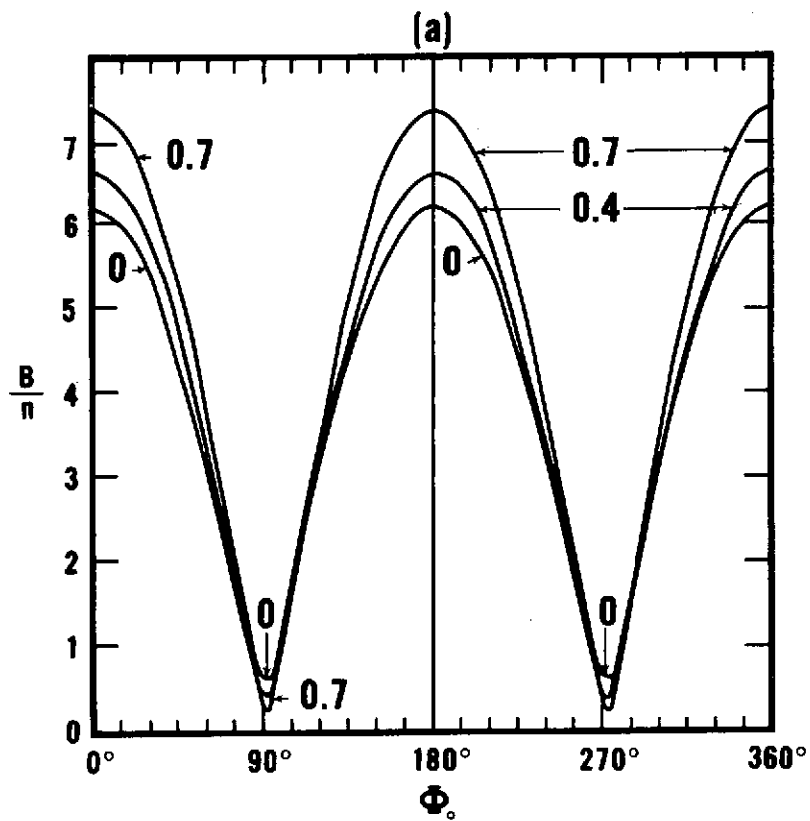






1 AU





0.3 AU

